Rock-physics joint inversion of resistivity-log and seismic velocity for hydrate characterization

Diana Sava, Bob Hardage, Paul Murray, and Mike DeAngelo*
Bureau of Economic Geology, Jackson School of Geosciences, The University of Texas at Austin, Austin TX

Summary

We present a method for joint inversion of electrical resistivity measurements and velocity data for estimating gas-hydrate concentration in deep-water environments. Our technique is based on a Bayesian approach and combines rock-physics elastic theories and empirical relations for electrical resistivity with stochastic simulations to account for the natural variability of the petrophysical parameters involved in the inversion.

Most gas-hydrate systems found in deep-water, near-seafloor strata in the Gulf of Mexico have to be described with limited data because the intervals over which companies acquire logs and cores involve only reservoirs below the gas hydrate stability zone (GHSZ). The usual well-log information acquired over the GHSZ is restricted to gamma-ray and electrical resistivity logs. Also, only sparse geotechnical data are available from which porosity and lithology information can be obtained for near-seafloor strata. When we estimate gas-hydrate concentration in deep-water environments, we must take into account the inherent uncertainty associated with our predictions because of these data limitations. Our method allows us to estimate not only the hydrate concentration from simultaneous inversion of electrical resistivity log and seismic velocity, but also provides a measure of the uncertainty associated with our predictions. By combining electrical resistivity and seismic velocity we can better constrain hydrate concentration and distribution within sediments, and we can reduce the inherent uncertainty associated with our predictions. We illustrate the methodology using examples from Green Canyon, GOM.

Introduction

Gas hydrates increase both the elastic moduli and the electrical resistivity of the sediments in which they occur (Collett, 2001). However, the relation between hydrate concentration, resistivity and velocity of strata containing hydrates is non-unique and uncertain. Some of these sources of uncertainty are related to data-measurement errors, limited availability of data (such as no density or neutron-porosity) , poor understanding of how hydrate is distributed among sediment grains, unexpected spatial variability of rock properties, and inadequate understanding of numerous other physical conditions and processes associated with hydrate systems. Therefore, by combining quantitatively the various types of hydrate-sensitive information we can better constrain our predictions about gas hydrate distribution. Our methodology for joint inversion uses a Bayesian (Bayes, 1783) approach and combines rock-physics theories and empirical relations with stochastic simulations. We show examples of estimating gas-hydrate concentration and the uncertainty associated with the estimates using electrical resistivity logs and 4C OBC seismic data at calibration wells.

Forward modeling of C_{GH} -R -V_P joint relation

In this section we discuss the forward modeling problem, which has as an outcome the joint theoretical relation between hydrate concentration, electrical resistivity, and velocity of sediments. Based on this joint theoretical relation, calibrated to our study area, we can then estimate hydrate concentrations using actual electrical resistivity and seismic velocity data at well locations.

Both electrical resistivity and elastic properties of hydrate-bearing sediments depend on sediment porosity (ϕ) and on hydrate concentration (C_{GH}) in pores. Therefore, we can model the joint relation between hydrate concentration, resistivity and velocities using Archie Equation and the rock physics elastic model for unconsolidated sediments with load-bearing hydrates (Helgerud et al., 1999; Sava and Hardage, 2006).

Each parameter in our rock-physics elastic modeling, and in the Archie Equation (Archie, 1942), is expressed as a probability distribution function (PDF) to account for the uncertainty associated with it. The PDFs used in the modeling are either Gaussian distributions or uniform distributions. Gaussian distributions are used for parameters whose expected values are known or measured. The mean of the Gaussian function is the expected value of the parameter; the standard deviation defines the uncertainty associated with this expected parameter value. The expected values for parameters such as cementation exponent, geometric factor, resistivity of brine, volumetric fraction of clay, elastic properties of brine, coordination number, and effective pressure vary with depth. Therefore, their individual PDFs update with depth. Other parameters for which we use Gaussian distributions are the elastic moduli and density of the mineral grains, whose expected values are assumed from published laboratory results (Mavko et. al, 1998). The PDFs for the elastic properties of the mineral grains do not change with depth, unless detailed information about mineralogy is acquired.In contrast to a Gaussian distribution, a uniform distribution is used when a likely value for the parameter is challenging to estimate, but the range of its variability can be defined. A uniform distribution assumes that within the range of variability being considered, any value of the described parameter is equally probable. We use uniform distributions for the saturation exponent needed in the Archie Equation, critical porosity, elastic moduli and density of hydrates, and hydrate concentration. These parameters and their associated PDF do not vary with depth.

We refer to the parameters involved in both our rock physics elastic modeling and Archie Equation as common parameters. There are two of these common parameters: porosity (ϕ) and hydrate concentration (C_{GH}). We use a Monte Carlo procedure to draw values for these common parameters from their associated PDFs and then compute the corresponding velocity and resistivity values using Monte Carlo draws from the PDFs for each of the parameters that are required for elastic modeling and for Archie Equation. In this fashion we obtain many possible realizations of the functions that jointly relate hydrate concentration, resistivity, and seismic propagation velocity. This joint relation is non-unique, uncertain, and varies with depth. This theoretical relation of hydrate concentration, electrical resistivity, and velocity can be expressed mathematically also as a probability density function in a three-dimensional model space (C_{GH}, V_P, R). This model space is updated with depth.

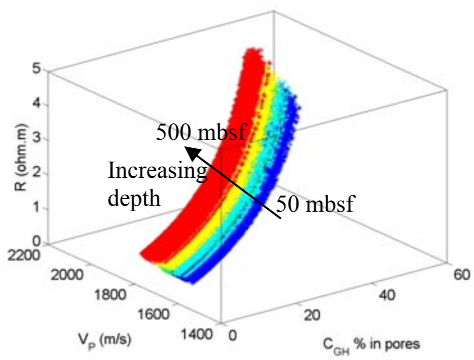

Figure 1. Monte Carlo simulations for the joint theoretical relation between hydrate concentration (C_{GH}), P-wave velocity (V_P), and resistivity (R). Data are color-coded by depth. The arrow indicates increasing depth over the gas hydrate stability zone.

Figure 1 presents the results for Monte Carlo simulations of the joint theoretical relation between hydrate concentration, P-wave velocity, and resistivity. The data are color-coded by depth, and the arrow indicates increasing depth within the gas hydrate stability zone (GHSZ). As expected, both electrical resistivity and P-wave velocity increase with increasing hydrate concentration and with increasing depth. At a fixed depth, the scatter in the data is caused by the uncertainty in the input parameters used in the elastic rock-physics model and Archie Equation. Based on these Monte Carlo realizations, we derive at each depth-step the joint theoretical PDF for hydrate concentration, P-wave velocity, and resistivity, generically denoted as $\xi(C_{GH}, V_P, R)$.

Joint inversion of electrical resistivity and velocity

A typical inversion problem has three different elements: 1) the *model parameters*, represented by the subsurface rock properties that we wish to detect and map (in this case, the hydrate concentration in the sediments), 2) the *data parameters* (e.g., seismic velocities and electrical resistivity measurements), and 3) the *physical laws* that relate the model parameters to the data parameters, which are given by *rock physics theories*, as discussed in forward modeling section.

To estimate hydrate concentration using seismic and resistivity data, we use a Bayesian approach formulated in the context of an inverse problem, as proposed by Tarantola (1987).

First, we express our prior information about hydrate concentration (information obtained before analyzing any seismic or resistivity data) as a PDF. We denote this prior PDF as $\Lambda_M(C_{GH})$, where subscript "M" stands for "model" parameter. In our study, this prior PDF is assumed to be a uniform distribution over all physically possible values for the hydrate pore-space fraction, meaning we allow this uniform distribution to range from 0% to 100%. However, this method allows us to introduce into this prior PDF for hydrate concentration any additional information available from other sources.

Second, we combine this prior PDF of hydrate concentration, $\Lambda_M(C_{GH})$, with information provided by seismic and resistivity measurements at calibration wells. Our prior information and any information obtained from seismic and resistivity data are assumed to be statistically independent. This assumption allows the prior joint PDF that combines hydrate concentration and data, $\Lambda(C_{GH}, V_P, R)$, to be written as

$$\Lambda(C_{GH}, V_P, R) = \Lambda_M(C_{GH})\, \Lambda_D(V_P)\, \Lambda_D(R). \quad (1)$$

In Equation 1, subscript "D" stands for data, and $\Lambda_D(V_P)$ and $\Lambda_D(R)$ are Gaussian PDFs that account for measurement uncertainties in the seismic P-wave velocity data and resisitivity log data we use in our hydrate inversion.

Third, we use Tarantola's (1987) strategy that states that the posterior PDF combining hydrate concentration and data, $\Psi(C_{GH}, V_P, R)$, is proportional to the prior joint PDF for hydrate concentration and data, $\Lambda(C_{GH}, V_P, R)$, multiplied by the joint theoretical PDF, $\xi(C_{GH}, V_P, R)$, which we derive using stochastic rock physics modeling, as presented in the previous section. Therefore, we can write:

$$\Psi(C_{GH}, V_P, R) = \Lambda(c_{GH}, V_P, R)\, \xi(C_{GH}, V_P, R). \quad (2)$$

From this posterior joint PDF, $\Psi(C_{GH}, V_P, R)$, we derive what is called the marginal distribution of hydrate concentration, $\Psi_M(C_{GH})$, by integrating the posterior joint PDF over velocity and resistivity data space. This marginal distribution, $\Psi_M(C_{GH})$, represents the posterior PDF for hydrate concentration in the pore space of the host sediment. From this posterior distribution we can derive the posterior expected value as our best estimate for hydrate concentration after integrating the resistivity and seismic information with depth-calibrated rock physics theories. At the same time, we also have a measure of uncertainty, given by the standard deviation of the posterior distribution on hydrate concentration.

Results

In this section we present results for estimating hydrate concentration across our study area in Green Canyon, Gulf of Mexico, where geotechnical borings and seafloor outcrops give hard evidence for the presence of hydrate.

Figure 2 presents on the left panel the seismic P-wave interval velocities determined with a raytrace-based velocity analysis technique at Well A (DeAngelo et. al, 2008). This method provides accurate interval velocities. The middle panel presents the electrical resistivity, logged while drilling (LWD). On the left and middle panels we superimpose the computed baselines for P-wave velocity and electrical resistivity of 100% brine saturated sediments (gray curves). These baselines were derived using the available information about porosity, lithology, brine salinity, and assuming hydrostatic pore pressure and normal geothermal gradient. We observe that both the seismic P-wave velocity and the electrical resistivity log show larger values than their corresponding baselines within the interval from 50 to 250 mbsf. This interval is interpreted to be hydrate-bearing because the presence of hydrates increases both the velocity and the electrical resistivity of their host sediments. We also observe that below this interval, the seismic P-wave velocity drops significantly below the baseline for 100% brine-saturated sediments. This interval is interpreted as being charged with free gas because gas is known to lower the P-wave velocity significantly. Therefore, the base of hydrate stability zone (BHSZ) at this well is interpreted to be approximately 250 m below the seafloor, as represented by the horizontal line in Figure 2. The electrical resistivity log shows resistivity values higher than the baseline below the BHSZ. This response is present because free gas and hydrates are both non-conductive phases, and an electrical resistivity log cannot differentiate between these two resistive components. However, P-wave velocity can distinguish between hydrate and free gas. Therefore, combining seismic information with electrical resistivity measurements helps reduce the ambiguity about hydrate distribution within sub-seafloor sediments.

The third panel in Figure 2 presents the posterior expected value (gray curve) from electrical resistivity log data for the saturation of the non-conductive phase, be that phase hydrate or free gas. Superimposed on the same panel is the expected estimate for hydrate concentration determined independently from the seismic interval P-wave velocities over the interval from 50 m to 250 m below the seafloor. These estimates assume that the hydrates are disseminated and load-bearing within that interval. We observe a good agreement between the estimates for hydrate concentration determined from electrical resistivity log and independently from the P-wave velocity. This agreement suggests that a good calibration was determined for the parameters that enter into both the Archie Equation and the rock physics elastic model. It also suggests that the assumption of load-bearing hydrates may be representative of the real-Earth hydrates at this location.

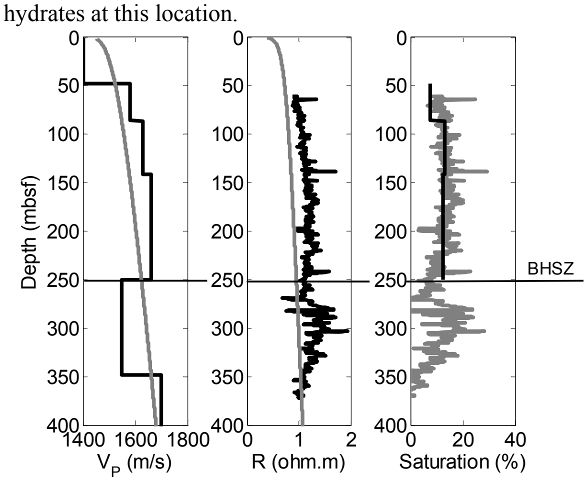

Figure 2. Well A: Seismic P-wave interval velocities (left panel) and electrical resistivity log (middle panel) with their corresponding baselines for brine-saturated sediments (gray curves). The posterior expected value for saturation of the non-conductive phase (either hydrate or free gas) determined from electrical resistivity log data is shown as the gray curve on the right panel. Superimposed on the right panel are the expected values for hydrate concentration, based on the P-wave interval velocities.

Seismic interval velocities have significantly lower resolution than the electrical resistivity logs. Therefore, for our joint inversion procedure, we use the average value for resistivity over each seismic velocity interval within the gas hydrate stability zone and we get an overall estimate for each of these intervals between 50 and 250 mbsf.

Figure 3 presents the posterior probability distribution functions (PDFs) for gas hydrate concentration in Well A for the following three P-wave velocity intervals within the GHSZ: between 50 m and 80 m (upper panel), between 80 m and 140 m (middle panel), and between 140 m and 250 m (lower panel). The dashed dark gray curves correspond to the posterior PDFs obtained from resistivity log inversion (assuming an average value for resistivity log over the specified intervals). The dotted lighter gray curves correspond to the posterior PDFs obtained from seismic P-wave velocity inversion. The black solid curves correspond to the posterior PDFs from the joint inversion of resistivity and seismic P-wave interval velocity. The results for the posterior expected values for hydrate concentration and their associated standard deviations for each of the intervals considered in Well A are summarized in Table 1. As expected, we find that the uncertainty associated with hydrate concentration reduces when a joint inversion is done using both velocity and resistivity data, compared to the uncertainty that is obtained when using velocity or resistivity information alone. The standard deviations associated with the estimates derived from the joint inversion are smaller than those associated with the individual estimates from resistivity or velocity separately.

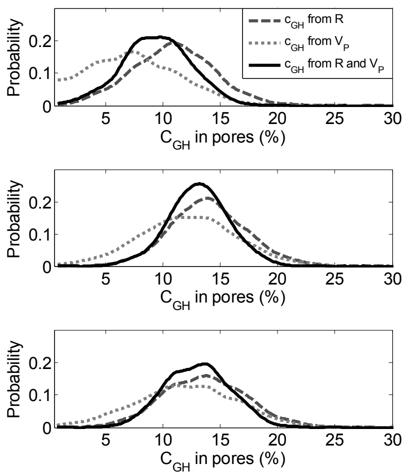

Figure 3. Posterior PDFs for gas hydrate concentration for the three velocity intervals in Well A: 50m-80m (upper panel), 80m-140m (middle panel), and 140m-250m (lower panel). The dashed darker gray curves are the posterior PDFs from resistivity log inversion (assuming an average value for resistivity log over each seismic P-wave intervals). The dotted lighter gray curves are the posterior PDFs from the seismic P-wave velocity inversion. The black solid curves are the posterior PDFs of the joint inversion of the blocked resistivity and P-wave velocity.

Table 1. Results for the posterior expected values (mean) and the associated standard deviation (std.) for hydrate concentration in sediment pores (C_{GH}) for the tree seismic interval velocities in Well A.

WELL A	C_{GH} from R		C_{GH} from V_P		C_{GH} from R and V_P	
Seismic intervals	mean (%)	std. (%)	mean (%)	std. (%)	mean (%)	std. (%)
50- 80m	11.12	3.65	7.34	4.1	9.39	2.98
80-140m	14.02	3.39	12.51	4.3	13.34	2.71
140-250m	13.62	3.66	12.08	4.4	12.98	2.88

Conclusions

We have presented a joint inversion methodology of electrical resistivity and P-wave velocity for estimating gas-hydrate concentration in sediments from deep-water, near-seafloor strata. This technique uses a Bayesian approach and combines rock-physics elastic theories and empirical relations for electrical resistivity with stochastic simulations. All of the parameters involved in relating hydrate concentration to electrical resistivity and velocity are expressed as probability distribution functions, which vary with depth below the seafloor. Therefore, using this method we accounted for the variability in the elastic properties of the mineral, hydrate, and fluid constituents of near-seafloor sediments, as well as for the variability in brine resistivity, cementation exponent, and all other petrophysical parameters required for our joint inversion of resistivity and seismic velocity to hydrate concentration. At the same time, our technique allowed us to estimate the uncertainty associated with the final results for hydrate concentration. We showed that by combining electrical resistivity measurements with seismic velocity we we can reduce the uncertainty associated with our predictions.

This quantitative integration of electrical resistivity and P-wave velocity is especially critical for estimating hydrate concentration in deep-water near-seafloor strata, where there is limited availability of well-log data. The typical well-logs across hydrate stability zones in our study area are restricted to gamma-ray and electrical resistivity, which cannot differentiate between nonconductive gas-hydrate and free gas in pores. In contrast, P-wave velocity can distinguish between hydrates and free gas and a joint inversion better constrain the hydrate concentration and distribution.

Based on the examples from Green Canyon presented in the paper, we concluded that a careful calibration of both electrical and elastic properties of sediments from deep-water, near-seafloor strata can yield similar results for hydrate concentration estimated independently from electrical resistivity and from seismic velocity. The good agreement between the independent estimates of hydrate concentration from resistivity-log and seismic velocity at well locations suggests the validity of a load-bearing-hydrate assumption in marine sediments. This agreement between independent estimates of hydrate concentration from electrical resistivity and from seismic velocity at calibration wells will allow us to make predictions of hydrate concentration based on velocity information alone away from the wells.

The joint inversion technique enabled us to make more reliable and better constrained predictions about hydrate concentration and distribution and to quantify the associated uncertainty, in the context of scarce availability of well-log data encountered in studying deep-water hydrate systems.

Acknowledgements

This research investigation was funded by the U.S. Department of Energy through contract DE-FC26-05NT42667.